Materials Sciences Research Journal 2008, Volume 2, Issue 3/4 ISSN 1935-2441
pp.145-167

INVESTIGATIONS ON FAILURES OF HYDROFORMING DEEP DRAWING PROCESSES

J. J. V. Jeyasingh[a], B. Nageswara Rao[*b] and A. Chennakesava Reddy[c]

[a]Mechanical Engineering Entity, Vikram Sarabhai Space Centre, Trivandrum-695022, India
[b]Structural Analysis and Testing Group, Vikram Sarabhai Space Centre, Trivandrum-695022, India
[c]Faculty of Mechanical Engineering, JNTU College of Engineering, Anantapur - 515 002, India

ABSTRACT

Flexible die forming technology has become more attractive for deep drawing process of sheet metals in recent years because of the substantial weight saving, cost reduction and quality improvement. This process helps to overcome some of the inherent problems faced in the conventional deep drawing process with rigid tools. As a result, there is an increasing need for analytical and numerical simulation of flexible die forming process to arrive at the optimum process parameters to achieve a defect free product. In a design process, it is very cost-effective to make the right decisions early. Satisfactory reliable simulations with the minimum input data can give much helpful information for these decisions. The details on a simple tooling developed to carryout the experimental trials and the process parameters are highlighted. Failures encountered during flexible die forming are presented in this paper.

Keywords: Hydroforming, Flexible die forming, Deep drawing.

NOMENCLATURE

a	Punch radius
$b,\ b_0$	Current blank radius, initial blank radius
h	Punch travel

[*] Corresponding author, E-mail: bnrao52@rediffmail.com; Phone: + 91- 471- 2565831; Fax : + 91- 471- 2564181

$k = \frac{\sqrt{\overline{R}}}{2}\sigma_e$	The maximum possible shear stress at $r = a$
n	Strain hardening exponent
$p,\ p_b, p_{cr}$	Fluid pressure, plastic buckling pressure, critical fluid pressure
$\overline{p}_{cr} = \frac{p_{cr}a}{\sigma_0 s}$	Normalized critical fluid pressure
$R = \frac{\dot{\varepsilon}_\theta}{\dot{\varepsilon}_s}$	Anisotropy value of the material
$\overline{R}$	$= \frac{2(1+R)}{(1+2R)}$
R_0	Radius of an arbitrary point on the blank which corresponds to an instantaneous radius 'r' in Zone-I
S	Blank thickness
T	Time
$u(r) = \frac{dr}{dt}$	Radial velocity
$u_0 = \frac{dh}{dt}$	Rigid zone velocity
$\dot{w}_{id}$	Ideal work rate
$\dot{w}_l$	Frictional work rate
$\dot{w}_\gamma$	Work rate of velocity discontinuity
$\dot{w}_p$	Energy rate of the surface traction
ε_r	Radial strain
$\dot{\varepsilon}_e$	Effective strain rate
$\dot{\varepsilon}_r, \dot{\varepsilon}_\theta,\ \dot{\varepsilon}_s$	Radial, tangential and normal strain rates
μ_1, μ_2	Frictional coefficients
$\overline{\mu}$	$= \frac{\mu_1 + \mu_2}{2}$
$\mu_1\, p\,,\ \mu_2\, p$	Interfacial shear stresses on the two faces of the flange
ρ	Current blank radius of curvature at the lip
σ_e	Effective stress
$\sigma_r, \sigma_\theta, \sigma_s$	Radial, tangential and normal stress components
$\sigma_0,\ \varepsilon_0$	Material constants in equation (4)
τ	Frictional force

1. INTRODUCTION

Hydroforming is a metal bending process that relies on fluid pressure, usually oil, to shape the metal piece. First, the metal piece to be formed is placed in a blank holder over the punch. The blank holder and punch are then moved next to the fluid filled dome. Pressure inside the dome is increased to form the work piece. As the punch moves against the diaphragm of the dome, the pressure inside the dome is adjusted to form the work piece to the desired shape. In some cases, the dome is moved while the punch stays stationary until it is ready to form the part, but the basic mechanics remains the same [1, 2]. Deep drawing, using the Hydroforming method, requires only a draw ring (blank holder) and male punch. No die maker's fit is necessary. Set-ups are quick and simple. The tooling is self-centered and self-aligning. The flexible diaphragm minimizes and often eliminates shock lines and draw marks normally created by matched die forming. Because pressures can be controlled over the entire blank, a higher percentage of reduction is possible and material thinout can be kept to a minimum. Two or three conventional deep draw operations can often be replaced by one operation using the Hydroform method.

Tirosh et al. [3] have demonstrated that failure by rupture results from excessive fluid pressure, whereas the failure by wrinkling results from insufficient fluid pressure. It is plausible, therefore, that a pre-determined pressure-path which maneuvers between these bounds may result in perfect products. These assertions have motivated a more specific analysis of buckling occurrences [4] on the one hand and rupture occurrences [5] on the other hand. Yossifon and Tirosh [6] have investigated the suppression of buckling phenomenon at the flange area, using lateral hydrostatic fluid pressure in place of rigid blank-holder. The geometrical and material constraints which limit the quality of hydroforming products in regard to failure by wrinkling (buckling) and/or rupture (tensile stability) are investigated in a unified framework [7]. The analysis is based on the theorems of plasticity (with a power-law hardening and Mises-Hill normal anisotropy) and resulted in distinct bounds for the permissible operating fluid pressure path. The process of hydrodynamic deep-drawing has been modified to draw tapered blanks of small angles. This option, unattainable in classical deep drawing processes, has its applications in producing specially-dedicated products [8]. The concept of maximum drawing ratio, supplementary to the well-known limit drawing ratio, is defined, examined, and illustrated by experiments [9]. Yossifon and Tirosh [10] have been made an attempt to structure a solution which will enable one to predict the final dimension of hydroforming products for a wide family of constitutive behavior of the sheet blanks (including strain hardening and normal anisotropy). Shirizly et al. [11] have utilized a hydro-mechanical deep drawing process to study the roles played by die curvature, interfacial friction, material hardening, etc. in deep drawing performance. Their analytical study is based on limit analysis in plasticity (applying both the upper and the lower bounds simultaneously) with a special emphasis on the geometry of the die profile. It is shown that, in general, the greater the curvature, the lower is the punch load with some shift in the peak along the loading path. So, the incorporation of the die radius of curvature in sheet-forming analysis seems to be essential in describing the drawing process more realistically.

Park and Cho [12] have considered a tracking control of hydroforming pressure which is used for precision forming of sheet metals. The experimental results show that their proposed fuzzy self-learning controller can guarantee good tracking performance. Dohmann and Harti

[13] have set out the correlation between the tool construction, the tube and the process parameters for hydroforming processes. Noh and Yang [14] have proposed a simple kinematically admissible velocity field for hydroforming of arbitrarily-shaped boxes in which the punch surface can be described analytically. An initially circular blank is hydroformed into an elliptic circular box in the experiment considering the computed pressure versus punch stroke curve. Their methodology is validated by measuring the thickness variation. It is noted from the studies of Tirosh et al. [15] that the process can reach higher drawing ratios with substantially less assisted fluid pressure by controlling the temperature and/or the operating speed for restricting the changes in the material properties.

Novotny and Hein [16] have outlined the process window, special requirements and potentials of the hydroforming of sheet metal pairs, using sheet materials from heat treatable aluminum alloys. The increasing application of hydroforming techniques for the production of automotive lightweight components is mainly due to the attainable advantages regarding part properties and to the improving technology of the forming equipment. The presentation by Luke et al. [17] shows some examples of process development possibilities and describes the process technology and the performance of series production hydroforming lines, processing longitudinally welded aluminum tubes. Anwar Kandil [18] has been carried out an experimental program to study the effect of process parameters. Lang et al. [19] have proposed hydro-mechanical deep drawing with uniform pressure on the blank and investigated the characteristics of sheet hydroforming. With consideration of the forming limit diagram, the forming process was studied in simulation. The results from a simulation were in reasonable agreement with those from an experiment. To explore sheet deformation under complex strain conditions, the forming process of a conical cup was studied by analyzing the failure types including fracture and wrinkling [20].

Hydroforming can be subdivided into panel hydroforming and tubular hydroforming according to the blanks used. In hydroforming deep drawing process the sheet material undergoes large deformation and its flow is controlled by the process parameters as well as material properties. The process parameters include the initial pressure inside the pressure container, forming pressure during the pressure forming process, drawing load, drawing ratio and punch geometry. Figure 1 illustrates the principle of Hydroforming Process. Some of the difficulties surrounding this process are the pressures involved in forming the piece. Because the pressures involved are usually three to four times of those normally associated with deep drawing, careful attention should be paid to the pressure vessel so that none of the fluid leaks. If too little pressure is applied, the part will wrinkle, resulting in poor quality. If too much pressure is applied, the blank will shear and the part will have to be scraped. A very few theoretical analysis of the Hydroforming drawing process is available in the open literature [3-10].

1.1. Objective of the Present Study

Though there are potential technological advantages, there are some difficulties in systemizing the process parameters such as selection of proper die pressure to punch stroke, material behavior, etc. during the forming process. Lacking such solutions, tedious procedures are being followed to generate the process curves through trial and error methods. Thus repeatability of product configurations is not guaranteed.

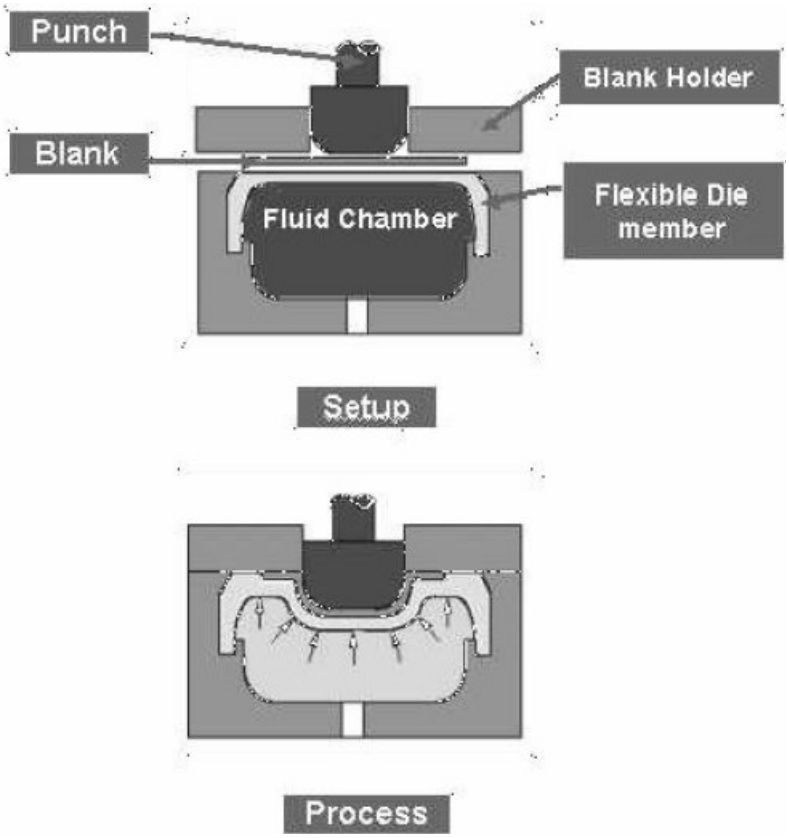

Figure 1. Schematic representation of Hydroforming principle.

In the absence of generalized models, an experimental approach was adopted to optimize the process parameters for realizing a defect free product of aerospace materials. The objective of this paper is to select and present simple and realistic analytical models for specifying the allowable fluid pressure path to avoid defect formation in the products through hydroforming deep drawing process. Test data [7, 9] of Al-1100, Copper, SS 304 L and Steel 1100 are considered to validate the selected models. Experiments were carried out on Inconel 718 and Copper materials to confirm further the applicability of the above analytical models.

2. ANALYTICAL MODELING

The domain of plastic flow during the hydroforming process is considered for convenience in three distinct zones as shown in Figure 2.

Zone - I: The flange area, which stays in contact with the die.
Zone - II: The blank curvature at the entrance to the cylindrical portion contact free from the die or punch
Zone - III: The cylindrical portion of the drawing cup, which is in firm contact (due to surrounding pressure) with the punch.

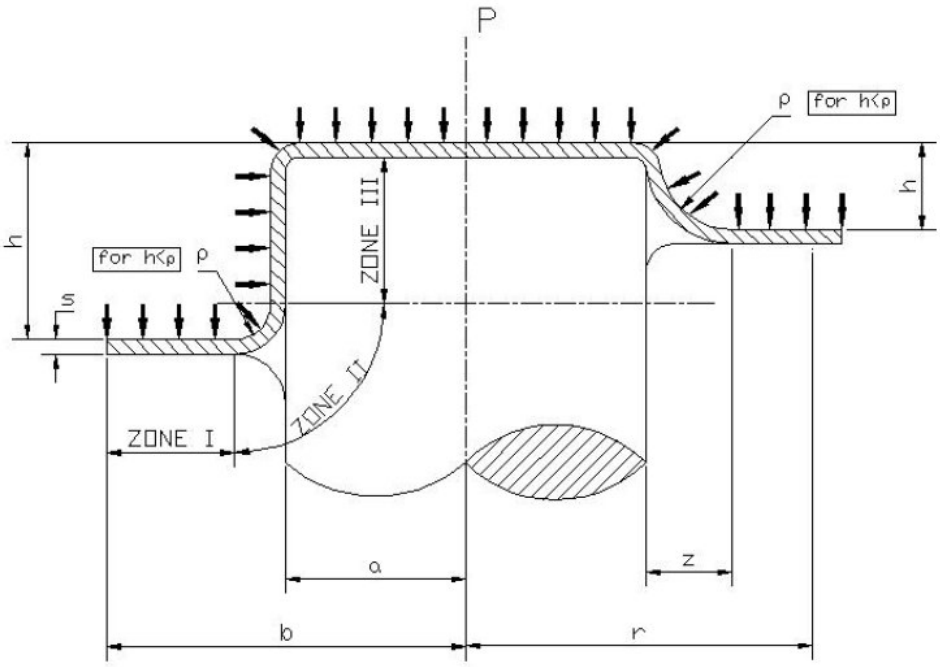

Figure 2. Different plastic zones during hydroforming.

The first two zones undergo large plastic deformation with nearly constant strain ratio. The third one is assumed to move with the punch as a rigid body, since the confining pressure restricts the flow by inducing shear resistance between cup walls and the punch. The stress analysis of Zone - I and Zone – II is required to understand the failure phenomenon of deep drawing processes.

The geometrical and material constraints which limit the quality of hydroforming products in regard to failure by wrinkling (buckling) and / or rupture (tensile instability) are to be well understood. It is essential to develop / select analytical models for the allowable fluid pressure path between bounding curves, viz. the upper curve below which the rupture is not likely to occur and the lower curve above which wrinkling is not likely to occur.

The constitutive equations for a material with normal anisotropy $\left(R = \frac{\dot{\varepsilon}_\theta}{\dot{\varepsilon}_s} \right)$ are:

$$\frac{\dot{\varepsilon}_r}{(1+R)\sigma_r - R\sigma_\theta - \sigma_s} = \frac{\dot{\varepsilon}_\theta}{(1+R)\sigma_\theta - R\sigma_r - \sigma_s} = \frac{\dot{\varepsilon}_t}{-(\sigma_r + \sigma_\theta - 2\sigma_s)} = \frac{\dot{\varepsilon}_e}{(1+R)\sigma_e} \qquad (1)$$

where the effective strain rate is defined (from the second strain rate variant) as:

$$\dot{\varepsilon}_e = \frac{1+R}{\sqrt{1+2R}} \sqrt{\dot{\varepsilon}_r{}^2 + \frac{2R}{1+2R}\dot{\varepsilon}_r\dot{\varepsilon}_\theta + \dot{\varepsilon}_\theta{}^2} \qquad (2)$$

In addition,

$$\varepsilon = \int \dot{\varepsilon}\, d(time) \quad or \quad \varepsilon_{ij} = \int \dot{\varepsilon}_{ij}\, d(time) \tag{3}$$

The uniaxial stress – strain behavior is described by

$$\sigma = \sigma_0 (\varepsilon_0 + \varepsilon)^n \tag{4}$$

where σ_0, ε_0 are material constants, $n =$ strain hardening exponent, $\sigma_r =$ radial stress in Zone- I, $\sigma_\theta =$ tangential stress in Zone – I and II, σ_s = normal stress (collinear with the fluid pressure direction), $\dot{\varepsilon}_r$, $\dot{\varepsilon}_\theta$, and $\dot{\varepsilon}_s$ are radial, tangential and normal strain rates.

From equation (1),

$$\dot{\varepsilon}_r - \dot{\varepsilon}_\theta = \left(\frac{1+2R}{1+R}\right)\frac{\dot{\varepsilon}_e}{\sigma_e}(\sigma_r - \sigma_\theta) \tag{5}$$

Assuming that the blank thickness remains constant, the incompressibility leads to

$$\dot{\varepsilon}_r = -\dot{\varepsilon}_\theta \tag{6}$$

Using equation (6) in (2) one gets,

$$\dot{\varepsilon}_e = \sqrt{\overline{R}}\,\dot{\varepsilon}_r \tag{7}$$

where $\overline{R} = \dfrac{2(1+R)}{1+2R}$

using equations (5) and (6), one gets

$$2\dot{\varepsilon}_r = \left(\frac{1+2R}{1+R}\right)\frac{\dot{\varepsilon}_e}{\sigma_e}(\sigma_r - \sigma_\theta) \tag{8}$$

From equations (7) and (8), one gets

$$\sigma_r - \sigma_\theta = \sqrt{\overline{R}}\,\sigma_e \tag{9}$$

Following the concepts of Tirosh et al [3], the generation of fluid pressure path through the plastic limit analysis in terms of the geometry of the product, the work hardening of the material and the frictional co-efficient is described below.

The overall area (A) of the work piece upto radius 'r' is:

$$A = \pi r^2 + 2\pi ah \tag{10}$$

where 'a' is the punch radius and 'h' is current travel of punch.

Differentiating equation (10) with respect to time, t

$$r\frac{dr}{dt} + a\frac{dh}{dt} = 0 \tag{11}$$

Defining the plastic zone radial velocity $u(r) = \frac{dr}{dt}$ and rigid zone velocity, $u_0 = \frac{dh}{dt}$, one can write equation (11) in the form

$$u = -a\frac{u_0}{r} \tag{12}$$

From equation(12), the radial strain rate is obtained as

$$\dot{\varepsilon}_r = \frac{du}{dr} = a\frac{u_0}{r^2} \tag{13}$$

Since strains are proportional, the total strain rate at any point in the flange region is

$$\varepsilon_r = -\int_{r_0}^{r} \frac{dr}{r} \tag{14}$$

then integration leads to

$$\varepsilon_r = \ln\left(\frac{\sqrt{r^2 + 2ah}}{r}\right) \tag{15}$$

2.1. Limit of Plastic Buckling Pressure

The ideal work rate ($\dot{w}_{id}$) and a general material with constant thickness is:

$$\dot{w}_{id} = \int_v (\sigma_r \dot{\varepsilon}_r + \sigma_\theta \dot{\varepsilon}_\theta) dv = \int_v (\sigma_r - \sigma_\theta) \dot{\varepsilon}_r dv$$

using equations (4), (9), (13) and $\varepsilon = \varepsilon_e = \sqrt{\overline{R}}\,\varepsilon_r$ in equation(4), one gets

$$\dot{w}_{id} = 2\pi\sqrt{\overline{R}}\, a s u_0 \sigma_0 \int_a^{\sqrt{b_0^2 - 2ah}} \frac{1}{r}\left\{\sqrt{\overline{R}} \ln\left(\frac{\sqrt{r^2 + 2ah}}{r}\right) + \varepsilon_0\right\}^n dr \tag{16}$$

where 'b_0'is the initial blank radius.

The frictional work rate ($\dot{w}_l$)is;

$$\dot{w}_l = \int \tau u(r) dS = 2\pi \int_a^{\sqrt{b_0^2 - 2ah}} \overline{\mu} p u_0 a dr = 2\pi\overline{\mu} p u_0 a\left[\sqrt{b_0^{\,2} - 2ah} - a\right] \tag{17}$$

Here 'τ' is the frictional force and p is the fluid pressure. $\overline{\mu} = \dfrac{\mu_1 + \mu_2}{2}$, $\mu_1\, p$ and $\mu_2\, p$ are the interfacial shear stresses on the two faces of the flange.

The work rate ($\dot{w}_\gamma$) of velocity discontinuity is

$\dot{w}_\gamma = \int k \Delta u dS_\gamma = k\sqrt{2} u_0 2\pi a s$, which implies that

$$\dot{w}_\gamma = \sqrt{2\overline{R}}\,\pi a s u_0 \sigma_0 \left[\frac{\sqrt{\overline{R}}}{2} \ln\left(1 + 2\frac{h}{a}\right) + \varepsilon_0\right]^n \tag{18}$$

where's' is the blank thickness. The maximum possible shear stress, k = $\dfrac{\sqrt{\overline{R}}}{2}\sigma_e$ at r=a. This implies that

$k = \dfrac{\sqrt{\overline{R}}}{2}\sigma_0 (\varepsilon_a + \varepsilon_0)^n$, where $\varepsilon_a = \dfrac{\sqrt{\overline{R}}}{2} \ln\left(1 + 2\dfrac{h}{a}\right)$

The Energy rate ($\dot{w}_p$) of the surface traction is

$$\dot{w}_p = \pi a^2 u_0 p \tag{19}$$

By using equations (16) to (19), the pressure path above which wrinkling does not occur can be obtained from

$$\pi\left(b_0{}^2 - 2ah\right)pu_0 = \dot{w}_{id} + \dot{w}_l + \dot{w}_\gamma + \dot{w}_p \tag{20}$$

which implies that

$$\frac{p_b}{\sigma_0} = \sqrt{\overline{R}}\,\frac{s}{A_3}\left(2A_1 + \sqrt{2}A_2\right) \tag{21}$$

Here $A_1 = \int_a^{\sqrt{b_0{}^2-2ah}} \frac{1}{r}\left\{\sqrt{\overline{R}}\,\ln\left(\frac{\sqrt{r^2+2ah}}{r}\right) + \varepsilon_0\right\}^n dr$

$$A_2 = \left\{\frac{\sqrt{\overline{R}}}{2}\ln\left(1+2\frac{h}{a}\right) + \varepsilon_0\right\}^n$$

$$A_3 = \left[\frac{b_0{}^2}{a} - a - 2\left\{h + \mu\left(\sqrt{b_0{}^2 - 2ah} - a\right)\right\}\right]$$

The limit of the plastic buckling pressure (p_b) can be obtained directly from equation (21) by specifying the punch travel ($\frac{h}{a}$).

2.2. Limit of the Rupture Pressure

Following the concepts of Yossifon and Tirosh [5], the critical fluid pressure path above which rupture by tensile instability may occur in the hydroforming deep drawing process is generated. The details of which are furnished below.

Consider the equilibrium equation in Zone-I with uniform frictional resistance $\overline{\mu}\, p$ as

$$\frac{d}{dr}\left(s\,\sigma_r\right) + \frac{s}{r}\left(\sigma_r - \sigma_\theta\right) + 2\,\overline{\mu}\, p = 0 \tag{22}$$

The effective flow stress induced on the blank during forming process can be written considering Tresca yield criterion as,

$$\sigma_r - \sigma_\theta = \sigma_{\max} - \sigma_{\min} = \sigma_e \tag{23}$$

The boundary condition at the end of the ring:

$$\sigma_r = -p \text{ at } r = b \tag{24}$$

Using equation (23) in (22) and applying the boundary condition (24), the radial stress distribution at the flange area (Zone-I): $(a+z) \le r \le b)$ is

$$\sigma_r^{\ I} = p\left[\frac{2\mu}{s}(b-r)-1\right] + \int_r^b \frac{1}{r}\sigma_0\left(\sqrt{\overline{R}}\varepsilon_r^{\ I} + \varepsilon_0\right)^n dr \tag{25}$$

and the corresponding hoop stress distribution can be obtained from

$$\sigma_\theta^{\ I} = \sigma_r - \sigma_e \tag{26}$$

From the volume constancy condition, the relationship between the current blank radius of curvature ' ρ ', punch travel 'h' and current blank radius 'b' can be written as

$$\left(\frac{b}{a}\right)^2 = \left(\frac{b_0}{a}\right)^2 - 2\frac{h}{a} - (\pi-4)\frac{\rho}{a} - (\pi-3)\left(\frac{\rho}{a}\right)^2 \quad \text{when h} \ge \rho \tag{27}$$

and

$$\left(\frac{b}{a}\right)^2 = \left(\frac{b_0}{a}\right)^2 + 2\frac{z}{a} + \left(\frac{z}{a}\right)^2 - 2\frac{\rho}{a}\left\{\left(1+\frac{z}{a}\right)\cos^{-1}\left(1-\frac{h}{a}\right) - \frac{h}{a}\right\} \quad \text{when h} \le \rho \tag{28}$$

where $z = \sqrt{2h\rho - h^2}$

Since the strain axis does not undergo rotation and so the radial strain $\varepsilon_r = -\int_{r_0}^{r} \frac{dr}{r}$ can be integrated along the radial path to yield

$$\varepsilon_r^{\ I} = \ln\left(\frac{G(r,h,\rho)}{r}\right) \tag{29}$$

Here $G(r,h,\rho)$ in equation (29) represents the radius 'r_0' of an arbitrary point on the blank which corresponds to an instantaneous radius 'r' in Zone-I.

From geometrical considerations, when $h \le \rho$ and $z = \sqrt{2h\rho - h^2}$:

$$G(r,h,\rho)=a\left[\left(\frac{r}{a}\right)^2-2\left(\frac{z}{a}\right)-\left(\frac{z}{a}\right)^2+2\left(\frac{\rho}{a}\right)\left\{\left(1+\frac{z}{a}\right)\cos^{-1}\left(1-\frac{h}{\rho}\right)-\frac{h}{\rho}\right\}\right]^{\frac{1}{2}} \tag{30}$$

when h $\geq \rho$ for which $z=\rho$,

$$G(r,h,\rho)=a\left[\left(\frac{r}{a}\right)^2-2\left(\frac{h}{a}\right)+(\pi-4)\left(\frac{\rho}{a}\right)+(\pi-3)\left(\frac{\rho}{a}\right)^2\right]^{\frac{1}{2}} \tag{31}$$

In the lip area (Zone-II), there is no interfacial shear as in Zone-I (no contact with die or ram in Zone-II) and considering the geometry, the equilibrium equation in Zone-II can be written as,

$$\frac{d\sigma_r}{dr}+\frac{\sigma_e}{r}=0 \tag{32}$$

Solving equation (32) with the initial condition $\sigma_r=\sigma_r{}^I(a+z)$ at $r=a+z$, the radial stress and strain can be written as (Zone-II: $a\leq r\leq a+z$):

$$\sigma_r{}^{II}=\sigma_r{}^I(a+z)+\int_r^{a+z}\frac{1}{r}\sigma_0\left(\sqrt{\overline{R}}\,\varepsilon_r{}^{II}+\varepsilon_0\right)^n dr \tag{33}$$

$$\varepsilon_r{}^{II}=\ln\left(\frac{F(r,h,\rho)}{r}\right) \tag{34}$$

For h $\leq \rho$, $z=\sqrt{2h\rho-h^2}$:

$$F(r,h,\rho)=a\left[1+2\frac{\rho}{a}\left\{\left(1+\frac{z}{a}\right)\left[\cos^{-1}\left(1-\frac{h}{\rho}\right)-\sin^{-1}\left(\frac{a+z-r}{\rho}\right)\right]\right\}+\frac{\rho}{a}\left\{1-\frac{h}{\rho}-\sqrt{1-\left(\frac{a+z-r}{\rho}\right)^2}\right\}\right]^{\frac{1}{2}} \tag{35}$$

For h $\geq \rho$, z = ρ:

$$F(r,h,\rho)=a\left[1+2\frac{h}{a}-2\frac{\rho}{a}\left\{1-\left(1+\frac{\rho}{a}\right)\left[\cos^{-1}\left(\frac{a+\rho-r}{\rho}\right)\right]+\frac{\rho}{a}\sqrt{1-\left(\frac{a+\rho-r}{\rho}\right)^2}\right\}\right]^{\frac{1}{2}} \tag{36}$$

A unique character of hydroforming process is that the fluid pressure causes a firm contact between the blank and the die and the ram. Since the fluid pressure plays the role of a blank holder, it should be pre-programmed to be at any instant high enough to prevent early buckling in the flange area. However, under certain conditions (i.e., with thin blanks at high

$\frac{b_0}{a}$ ratio's) the blank may fail by tensile rupture. Contrary to the classical deep drawing process, where rupture occurs at the bottom of the cup, in hydroforming process, the rupture takes place at the upper part of the cup just at the beginning of the lip.

The maximum possible axial stress along the cup wall is [5]

$$\sigma_z = \sigma_0 \left[\frac{1+R}{\sqrt{1+2R}} \right]^{n+1} n^n \tag{37}$$

Equating the axial stress in equation (37) to the radial stress at radius 'a' of equation (33), the critical fluid pressure (p_{cr}) at instability can be evaluated in terms of the material properties, the geometry of the cup and the average friction co-efficient as

$$\bar{p}_{cr} = \frac{p_{cr} a}{\sigma_0 s} = \frac{A_4 - A_5 - A_6}{A_7} \tag{38}$$

Here $A_4 = \left(\frac{1+R}{\sqrt{1+2R}} \right)^{n+1} n^n$,

$A_5 = \int_{a+z}^{b} \frac{1}{r} \left(\sqrt{\bar{R}} \varepsilon_r^{\ I} + \varepsilon_0 \right)^n dr$,

$A_6 = \int_{a}^{a+z} \frac{1}{r} \left(\sqrt{\bar{R}} \varepsilon_r^{\ II} + \varepsilon_0 \right)^n dr$, $A_7 = 2\frac{\mu}{a}\{b-(a+z)\} - \frac{s}{a}$ and $\bar{p}_{cr}$ is the normalized critical fluid pressure. It should be noted that $z = \sqrt{2h\rho - h^2}$ when h $\leq \rho$, whereas z = ρ when h $\geq \rho$.

The associated curvature at the lip is

$$\frac{\rho}{a} = \left\{ \frac{2\sigma_0 s}{p_{cr} a} \left(\frac{1+R}{\sqrt{1+2R}} \right)^{n+1} n^n + 1 \right\}^{\frac{1}{2}} - 1 \tag{39}$$

Here p_{cr} is a function of b_0, a, n, $\frac{s}{a}$, R, ε_0, h and ρ. The coupled non-linear equations (38) and (39) for p_{cr} and ρ have to be solved iteratively to obtain the limit of the rupture pressure. Initially, ρ has to be specified and obtain p_{cr} from equation (38). Use this value in equation (39) and update the ρ value. This iterative process has been carried out till the converged values of p_{cr} and ρ obtained. This way p_{cr} (rupture) curve is generated by

specifying the punch travel ($\frac{h}{a}$). The permissible fluid pressure path along the punch travel ($\frac{h}{a}$) will be above the plastic buckling pressure and below the rupture pressure.

3. VALIDATION THROUGH TEST RESULTS

In order to validate the permissible fluid pressure path along the punch travel, the test data [7,9] of Al-1100, Copper, SS304L and Steel 1100 are considered in the present study. The material properties, geometrical details and frictional conditions are given in Table 1.

Table 1. Geometrical details and material properties of cylindrical cups

Blank thickness s (mm)	Initial Blank radius b_0 (mm)	Punch radius a (mm)	Draw ratio $\frac{b_0}{a}$	Frictional Co-efficient $\bar{\mu}$
Al -1100 [9] : σ_0 =130 MPa; n=0.215, R = 0.8				
0.5	45	25	1.8	0.1
0.5	50	25	2.0	0.1
0.5	55	25	2.2	0.1
0.5	60	25	2.4	0.04
Copper [7] : σ_0 =320 MPa; n=0.15, R = 0.85				
1	125	78.125	1.6	0.2
SS 304 L [7] : σ_0 =1300 MPa; n=0.35, R = 1.0				
0.5	125	78.125	1.6	0.2
Steel 1100 [7] : σ_0 =500 MPa; n=0.25, R = 1.0				
0.8	125	78.125	1.6	0.2

The obtained buckling and rupture pressure boundaries are shown in Figures 3-9. The process pressure path followed for the tests and the corresponding quality of the products reveals that the boundaries of prediction are working fine based on which a safe pressure path can be selected for realizing a defect free product.

3.1. Experimental Study

The experimental setup consists of the Flexible die tooling and a 400 T conventional hydraulic press. A simple flexible tooling was developed, which can be placed on the work table of a conventional hydraulic press to carry out the hydroforming operation. Figure- 10 shows the tooling assembly developed and used for experiments. The Punch geometry is same as that of the product and designed to take the load acting on it. The die chamber is designed to withstand an operating pressure of 100 MPa during the forming process.

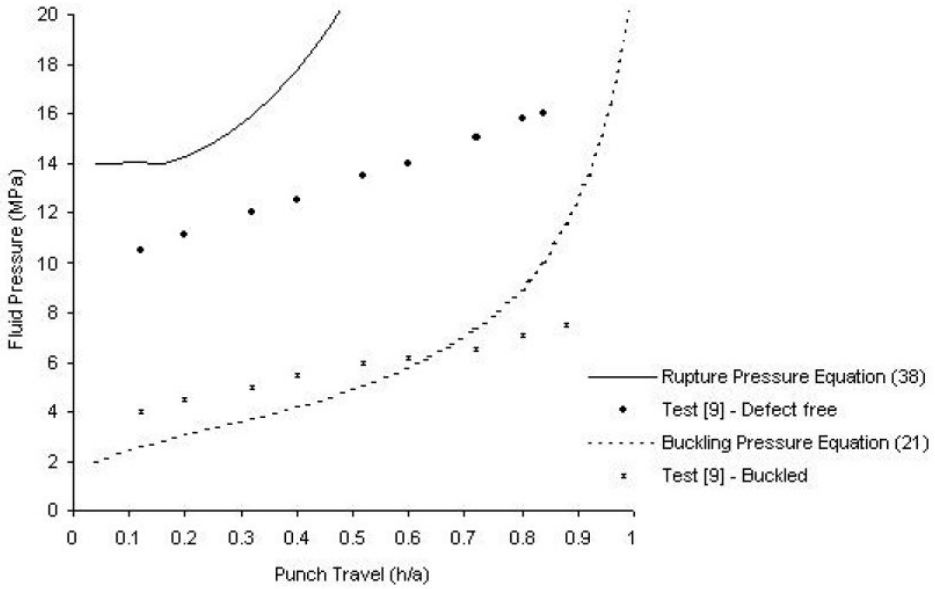

Figure 3. Rupture and Buckling limit curves for Al-1100, Draw ratio:1.8, s=0.5 mm, n=0.215, R=0.8, $\overline{\mu}$ =0.1.

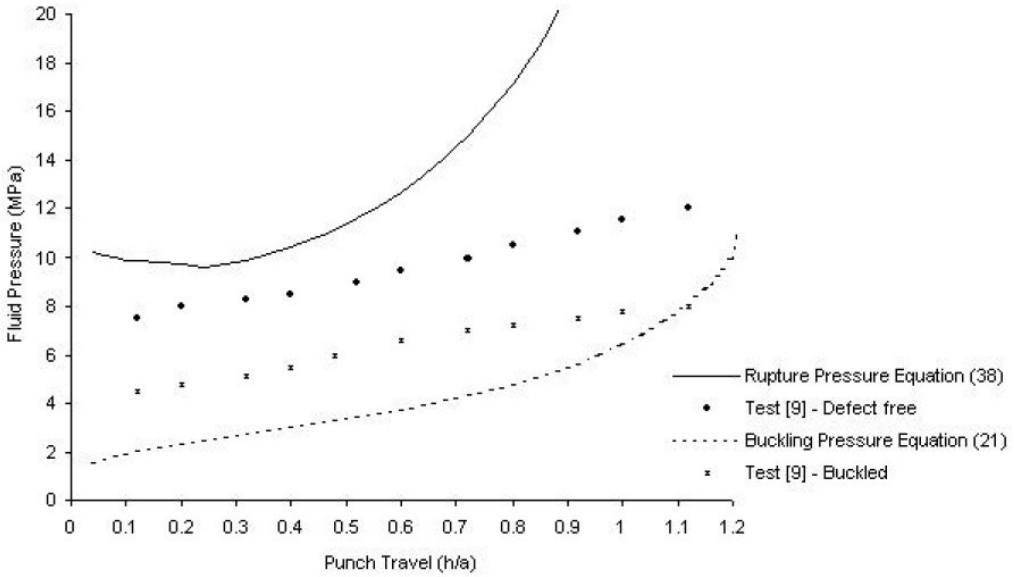

Figure 4. Rupture and Buckling limit curves for Al-1100, Draw ratio:2.0, s=0.5 mm, n=0.215, R=0.8, $\overline{\mu}$ =0.1.

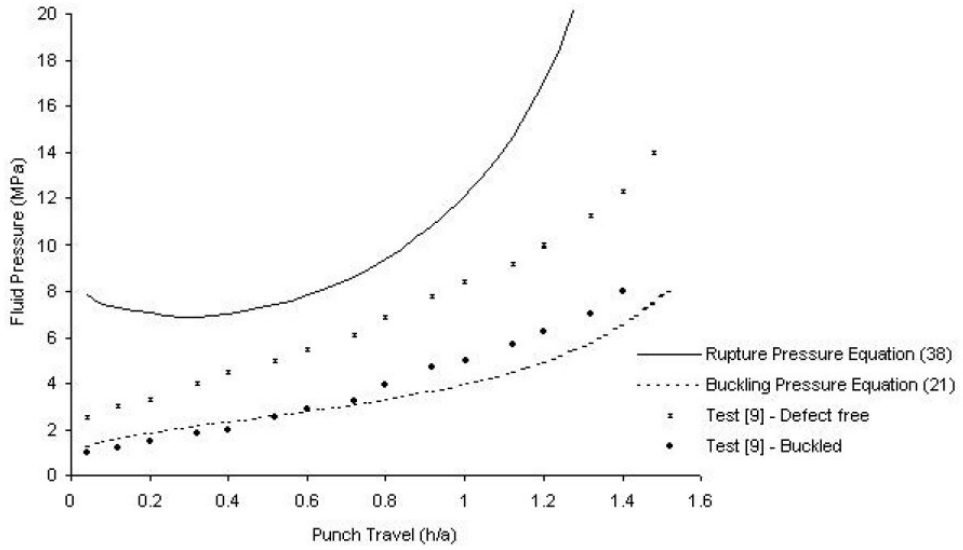

Figure 5. Rupture and Buckling limit curves for Al-1100, Draw ratio:2.2, s=0.5 mm, n=0.215, R=0.8, $\overline{\mu}=0.1$.

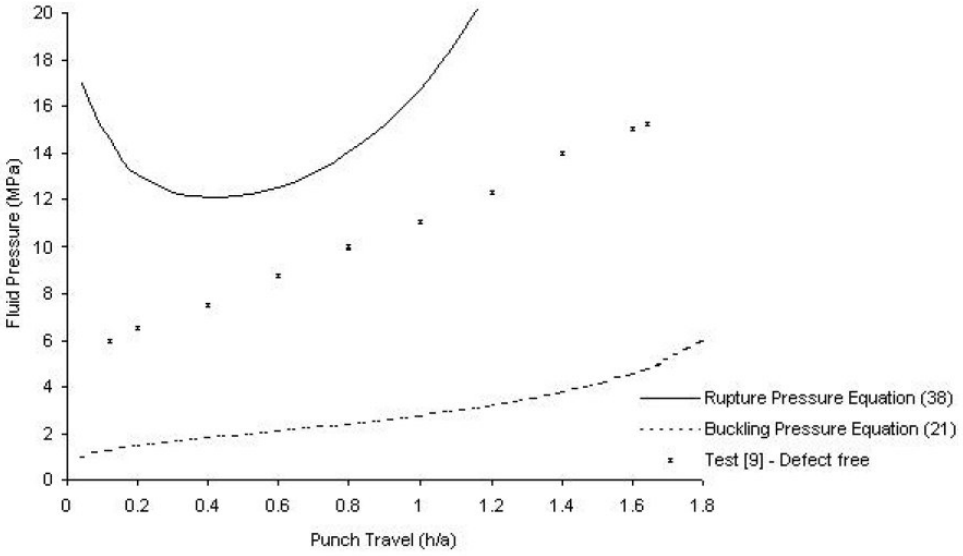

Figure 6. Rupture and Buckling limit curves for Al-1100, Draw ratio:2.4, s=0.5 mm, n=0.215, R=0.8, $\overline{\mu}=0.04$.

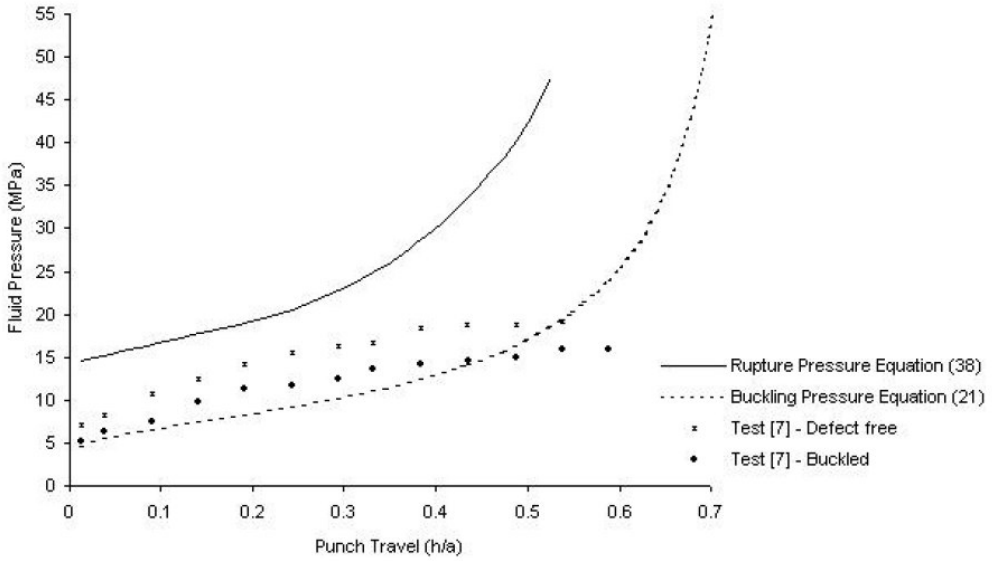

Figure 7. Rupture and Buckling limit curves for Copper, Draw ratio:1.6, s=1.0 mm, n=0.15, R=0.85, $\overline{\mu}$ =0.2.

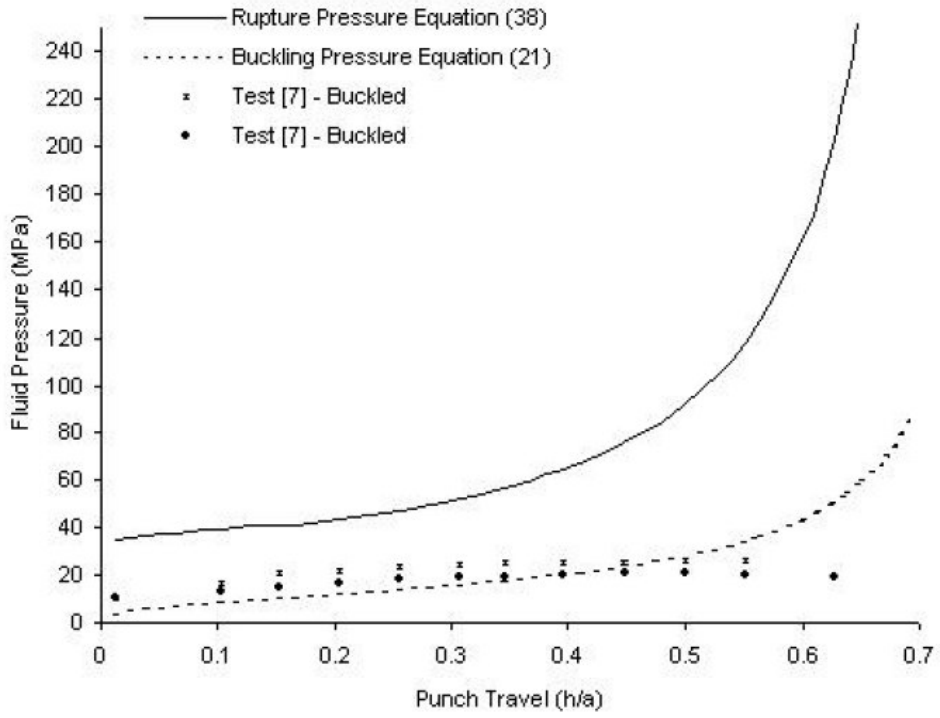

Figure 8. Rupture and Buckling limit curves for SS 304 L, Draw ratio:1.6, s=0.5 mm, n=0.35, R=1.0, $\overline{\mu}$ =0.2.

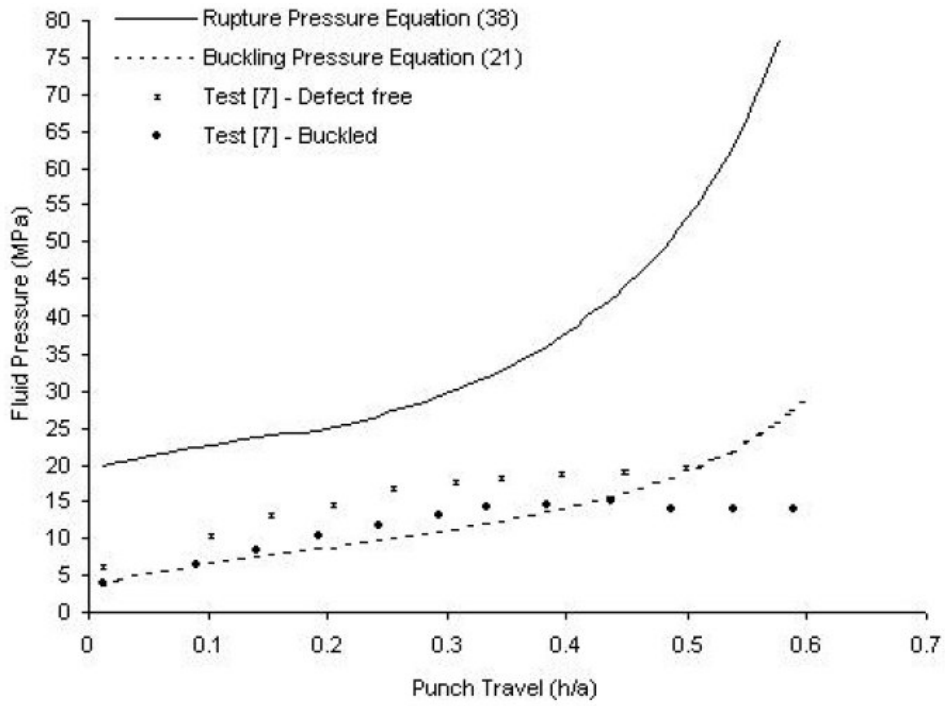

Figure 9. Rupture and Buckling limit curves for Steel 1100, Draw ratio:1.6, s=0.8 mm, n=0.25, R=1.0, $\overline{\mu}$ =0.2.

Figure 10. Tooling set up used for experiments.

The blank holder is designed such that required holding force can be exerted on to the flange either variable or constant during the entire forming process. The operating pressures are decided by the product material specification, its thickness and the geometry. To vary the process pressures, variable orifice was provided on the die chamber in the initial configuration which was improved by introducing proportional control hydraulic valves to regulate the fluid flow which controls the process pressures. Process control software was developed implementing the hydroforming process logic considering the tooling developed for conducting the experiments. The hydraulic control, Flexible die tooling and the data acquisition system were integrated together to achieve the present experimental set-up to carryout experiments.

The details of the material, geometry and the frictional conditions followed in the experimental study are given in Table-2. The product is a cylindrical cup with torispherical end dome. A diaphragm made of NBR rubber is used as the sealing element between the fluid chamber and the blank which acts as the flexible die during the forming process. Flange area of the blank is composed of two parts; the one which is pressed by the fluid against the die (rim area) and the second part (lip area) which stays contact free from the die. Experiments with different process parameters have been carried out. Initially, the pressing operations were carried out with zero pressure in the die. The variable orifice provided in the die acts as a pressure reliever during the pressing operation. Trial and error approach was followed during the experimental procedure to arrive at the optimum process parameters. The effect of die pressure on the blank holding as well as forming of the blank was studied by varying the process pressures. The rubber diaphragm of 5 mm thickness was used to facilitate easy wrapping against the punch under the backup pressure with required elongation and strength.

Table 2. Geometrical and material properties of Cylindrical torospherical end dome cups

Blank thickness s (mm)	Initial Blank radius b_0 (mm)	Punch radius a (mm)	Draw ratio $\frac{b_0}{a}$	Frictional Co-efficient $\bar{\mu}$
Inconel 718 : σ_0 = 1550 MPa; n=0.215, R = 0.94				
0.72	190	88.7	2.15	0.025
0.72	225	88.7	2.54	0.025
Copper : σ_0 = 320 MPa; n=0.15, R = 0.85				
1.0	190	88.7	2.15	0.025
1.0	225	88.7	2.54	0.025

3.2. Essence of Fluid Pressure Path

Figure 11 shows the buckling limit curve generated for Inconel-718 along with the specified pressure path. It can be seen from Figure 11 that the specified pressure path is intersecting the buckling limit curve. As a result, the products were buckled (see Figure 12). To validate the analytical modeling further, the buckling and rupture limit curves are

generated for the Copper material (see Figure 13). Since the specified pressure path during the experiments was within the buckling and rupture limit curves, good products were possible to realize (see Figure 14).

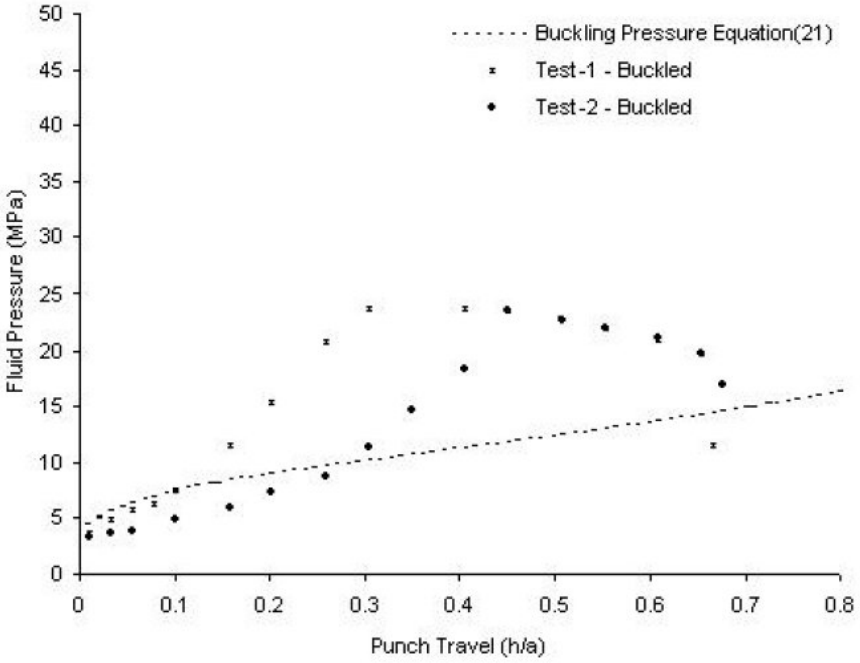

Figure 11. Rupture and Buckling limit curves for experimental material Inconel 718, Draw ratio:2.14, s=0.72 mm, n=0.215, R=0.94, $\overline{\mu} = 0.025$.

Figure 12. Wrinkling at the lip area(Zone- II) of Inconel-718 blank(Draw Ratio-2.14).

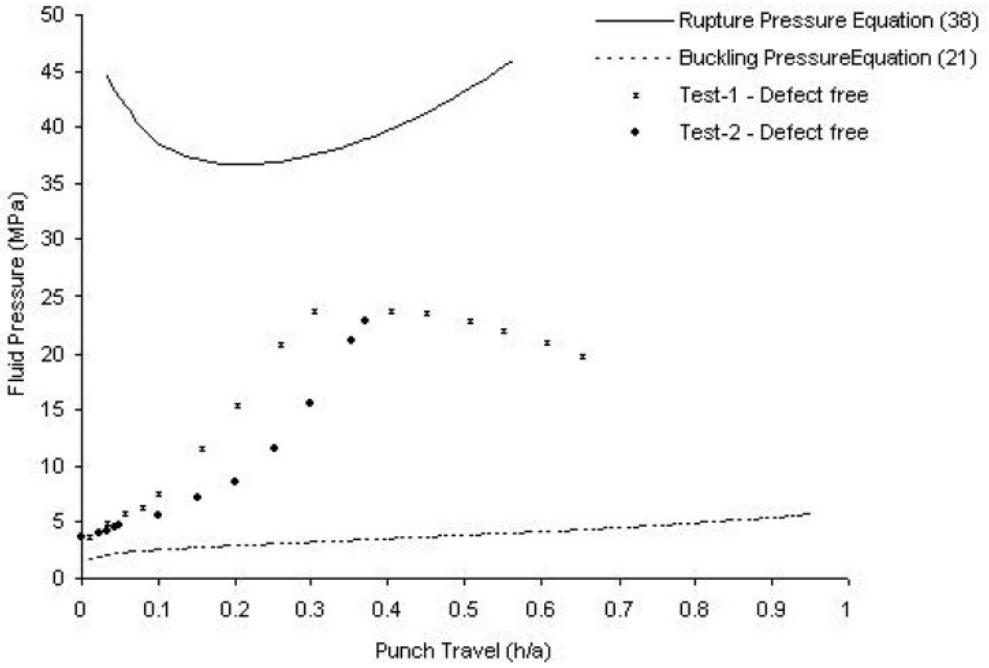

Figure 13. Rupture and Buckling limit curves for experimental material Copper, Draw ratio:2.14, s=1.0 mm, n=0.15, R=0.85, $\overline{\mu} = 0.025$.

Figure 14. Defect-free hydroformed Copper blanks with draw ratio 2.14.

3.3. Improved Facility Augmentation

Further, based on the above experience, the tooling design was improved to have data acquisition systems, hydraulic control elements and process control with the help of customized software implementing the optimized process logic.

CONCLUDING REMARKS

This paper highlights on the analytical modeling of the allowable fluid pressure path for obtaining defect-free product through hydroforming process. The models are validated through comparison of analytical and test results. The success of the process depends upon the pre-determined pressure supplied inside the die chamber during its trial out. The punch deforms the blank to its final shape by moving against a controlled pressurized fluid, which acts hydrostatically via a thin rubber diaphragm. As a result of the controllable backup pressure, a favorable pressure path, with respect to the punch travel, can be sought in order to delay the premature failures. The failure by rupture results from an excessive fluid pressure, while wrinkling results from insufficient fluid pressure. The range of pressure in between these two boundaries, give the working zone. It is subtended between two failure loci in which the pressure path can travel without causing failure.

ACKNOWLEDGEMENTS

The authors wish to thank: VSSC Editorial Board for making necessary arrangements for reviewing this article prior to its clearance for publication; Mr. R. Subramoniam (Deputy General Manager, Mechanical Engineering Entity), Dr. B. Sivasubramanian (Head, Computational Structural Technology Division) for their valuable comments / suggestions to improve the clarity of presentation; Mr. G. Kothandaraman (General Manager, Mechanical Engineering Entity), Dr. P.P. Sinha (Deputy Director) for their encouragements; and Dr. K. Radhakrishnan, Director, VSSC for giving permission to publish this article.

REFERENCES

[1] Richard L. Little, "*Metal Working Technology*", McGraw-Hill, New York (1977).

[2] D. Lascoe, "*Handbook of Fabrication Processes*", ASM International, Metals Park, Ohio (1988).

[3] J. Tirosh, S. Yossifon, R. Eshel and A. A. Betser, " Hydroforming process for uniform wall thickness products", *Trans. ASME Journal of Engineering for Industry*, Vol. 99, pp 685-691 (1977).

[4] S. Yossifon and J. Tirosh, " On suppression of plastic buckling in hydroforming processes", *International Journal of Mechanical Sciences*, Vol. 26, pp 389-402 (1984)

[5] S. Yossifon and J. Tirosh, " Rupture instability in hydroforming deep-drawing process", *International Journal of Mechanical Sciences*, Vol. 27, pp 559-570 (1985)

[6] S. Yossifon and J. Tirosh, " Buckling prevention by lateral fluid pressure in deep-drawing", *International Journal of Mechanical Sciences*, Vol. 27, pp 177-185 (1985)

[7] S. Yossifon and J. Tirosh, "On the permissible fluid-pressure path in hydroforming deep drawing processes – analysis of failures and experiments", *Trans. ASME Journal of Engineering for Industry*, Vol. 110, pp 146-152 (1988).

[8] J. Tirosh and A. Hazut, "The Hydrodynamic deep-drawing process for blanks of non-uniform thickness", *International Journal of Mechanical Sciences*, Vol.31, pp 121-130 (1989).

[9] S. Yossifon and J. Tirosh, " The maximum drawing ratio in hydroforming deep drawing processes", *Trans. ASME Journal of Engineering for Industry*, Vol. 112, pp 47-56 (1990).

[10] S. Yossifon and J. Tirosh, " On the dimensional accuracy of deep drawing products by hydroforming processes", *International Journal of Mechanical Sciences*, Vol. 33, pp 279-295 (1991)

[11] Shirizly, S. Yossifon and J. Tirosh, "The role of die curvature in the performance of deep drawing (hydro-mechanical) processes", *International Journal of Mechanical Sciences*, Vol.36, pp 121-135 (1994).

[12] H. J. Park and H. S. Cho, " A fuzzy self-learning control method with application to hydroforming processes", *Trans. ASME Journal of Engineering for Industry*, Vol. 117, pp 297-303 (1995).

[13] F. Dohmann and Ch. Hartl, "Hydrofoming – a method to manufacture light-weight parts", *Journal of Materials Processing Technology*, Vol.60, pp 669-676 (1996).

[14] T. S. Noh and D. Y. Yang, "A general formulation for hydroforming of arbitrarily-shaped boxes and its application to hydroforming of an elliptic – circular box", *Trans. ASME Journal of Manufacturing Science and Engineering*, Vol. 120, pp 481-488 (1998).

[15] J. Tirosh, A. Shirizly, D. Ben-David and S. Stanger, " Hydro-rim deep drawing processes of hardening and rate-sensitive materials", *International Journal of Mechanical Sciences*, Vol. 42, pp 1049-1067 (2000).

[16] S. Novotny and P. Hein, "Hydroforming of sheet metal pairs from aluminium alloys", *Journal of Materials Processing Technology*, Vol. 115, pp 65-69 (2001).

[17] H. U. Lucke, Ch. Hartl and T. Abbey, "Hydroforming", *Journal of Materials Processing Technology*, Vol. 115, pp 87-91 (2001).

[18] Anwar Kandil, " An experimental study of hydroforming deep drawing", *Journal of Materials Processing Technology*, Vol. 134, pp 70-80 (2003)

[19] L. Lang, J. Danckert and K. B. Neilsen, "Investigation into sheet hydroforming based on hydromechanical deep drawing with uniform pressure on the blank", *Proc. Instn Mech. Engrs. Part B : Journal of Engineering Manufacture*, Vol. 218, pp 833-844 (2004).

[20] L. Lang, J. Danckert and K. B. Neilsen, "Analysis of key parameters in sheet hydroforming combined with stretching forming and deep drawings", *Proc. Instn Mech. Engrs. Part B: Journal of Engineering Manufacture*, Vol. 218, pp 845-856 (2004).

Reviewed by
Mr. R. Subramoniam
Deputy General Manager, Mechanical Engineering Entity
Vikram Sarabhai Space Centre, Trivandrum – 695 022, India
and
Dr. B. Sivasubramanian
Head, Computational Structural Technology Division
Vikram Sarabhai Space Centre, Trivandrum – 695 022, India